INTERNATIONAL JOURNAL OF OPTIMIZATION IN CIVIL ENGINEERING
Int. J. Optim. Civil Eng., 2018; 8(1):137-158

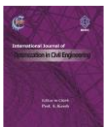

DAMAGE AND PLASTICITY CONSTANTS OF CONVENTIONAL AND HIGH-STRENGTH CONCRETE PART II: STATISTICAL EQUATION DEVELOPMENT USING GENETIC PROGRAMMING

M. Moradi[1], A. R. Bagherieh[1*, †] and M. R. Esfahani[2]
[1]*Department of Civil Engineering, School of Civil Engineering and Architecture, Malayer University, Malayer, Iran*
[2]*Department of Civil Engineering, Ferdowsi University of Mashhad, Mashhad, Iran*

ABSTRACT

Several researchers have proved that the constitutive models of concrete based on combination of continuum damage and plasticity theories are able to reproduce the major aspects of concrete behavior. A problem of such damage-plasticity models is associated with the material constants which are needed to be determined before using the model. These constants are in fact the connectors of constitutive models to the experimental results. Experimental determination of these constants is always associated with some problems, which restricts the applicability of such models despite their accuracy and capabilities. In the present paper, the values of material constants for a damage-plasticity model determined in part I of this work were used as a database. Genetic programming was employed to discover equations which directly relate the material constants to the concrete primary variables whose values could be simply inferred from the results of uniaxial tension and compressive tests. The simulations of uniaxial tension and compressive tests performed by using the constants extracted from the proposed equations, exhibited a reasonable level of precision. The validity of suggested equations were also assessed via simulating experiments which were not involved in the procedure of equation discovery. The comparisons revealed the satisfactory accuracy of proposed equations.

Keywords: reinforced concrete; genetic programming; constitutive modeling; continuum damage mechanics; plasticity.

Received: 20 April 2017; Accepted: 10 July 2017

[*]Corresponding author: Department of Civil Engineering, School of Civil Engineering and Architecture, Malayer University, Malayer, Iran
[†]E-mail address: bagheri@malayeru.ac.ir (A. R. Bagherieh)

1. INTRODUCTION

With the rapid development of technology, the need for more spacious and complex buildings is growing. Although the construction elements of concrete in conventional buildings are usually designed based on international design codes and simplified modeling, in taller and more complicated constructions, accurate modeling of the materials behavior for an optimal and safe design is of great importance. Even before applying any external load, there are many micro cracks in concrete, especially in the spaces between the coarse aggregates and mortar [1]. Development of these cracks during loading, leads to a non-linear behavior at low stress levels and volume dilations close to rupture. Regarding the complicated behavior of concrete, numerous experimental investigations using uniaxial and multiaxial tests including tensile, compression and cyclic loading have been conducted [2-7]. These investigations have shown that the concrete response includes the strain-softening/hardening, degradation of stiffness, volume dilation, anisotropy and irreversible deformations. Irreversible deformations and volume dilation can be explained by plasticity theory. However, macroscopic spread of the micro cracks results in degradation of the primary stiffness and reduction of the effective cross-section of the materials. It is very complicated to describe this phenomenon based on the classic plasticity [8]; consequently, the strain-softening branch cannot be well predicted based on plasticity models [8]. Continuum damage theory describes this behavior simply; on the contrary, the irreversible deformations and volume dilation cannot be achieved by this theory [9].

In order to accomplish the complete modeling of the concrete behavior and overcome the introduced problems, some models are achieved by combining the plasticity theory and continuum damage mechanics [10-15]. The models obtained from this combination can represent the concrete behavior with appropriate accuracy [16]. However, equations of the constitutive damage-plasticity models are commonly associated with unknown constants, while they need to be accurately defined for conformity of experimental and modeling results. In the relevant literature, these constants are generally calculated by the consistency of the modeling and experimental results [10-15]. It is very difficult for ordinary users to access the appropriate experimental results and find these constants through trial and error, which has greatly limited the use of these models despite their good results [16]. Thus, any model that has fewer constants is assessed as a more appropriate model. Sima et al. [16] presented an elastic-plastic-damage model for predicting the cyclic behavior of concrete. All the input data of this model were directly achievable based on the uniaxial experimental results; however, the model was only able to simulate the concrete under the cyclic loads [16]. To determine the numerical constants of an elastic-damage model, Wardeh and Toutanji [17] used the genetic algorithm optimization based on the experimental results. Despite achieving promising results, this modeling method could not describe the irreversible deformations of the concrete.

Therefore, having the literature meticulously considered by the researchers, it seemed necessary to take further steps to make the elastic-plastic-damage models more applicable. Based on the results of the uniaxial tension and compressive tests, Moradi et al. [18] (i.e. the first part of this companion study, published in the present journal) determined the material constants of the elastic-plastic-damage model developed by Voyiadjis and Taqieddin [14]

using the genetic algorithm method. These constants were obtained for 44 uniaxial experimental samples including conventional and high-strength concretes. Moradi et al. [18] showed that, by using these constants, uniaxial, cyclic and biaxial loading experiments could be simulated with relative success. showed that, using these constants, other tests representing the concrete behavior can be simulated with relative success. In the present work, genetic programming was used to propose direct relationships for predicting the damage and plasticity constants of the Voyiadjis and Taqieddin's elastic-plastic-damage model [14]. Direct estimation of these constants could help make this model more applicable.

2. GENETIC PROGRAMMING (GP)

Development of trainable and reliable artificial intelligence for modeling applied problems is very important when classic mathematics or statistical methods are unable to provide accurate models for the phenomena [19]. Genetic programming is one of the newest patterns in the research field of computational intelligence known as evolutionary computation [20]. GP is an evolutionary computational method, which solves the problems automatically so that users do not need to know or identify the form or structure of the response. In contrast to other smart computational methods such as the neural network, this method does not lead to a black box. The answer made by this method is an explicit mathematical equation [21].

The genetic programming method is used to produce clear and regular equations and has been used for many applications such as the exponential and classic regressions [22-23]. In this method, the mathematical equations are expressed using tree structure. Any equation in GP indicates an individual introduced with its own specific genetic sequence. In GP, a community is considered with different people and GP operators are used to produce next generations. Various operators have been introduced for this method, two standard forms of which include mutation and crossover.

- **Mutation operator**

To produce next generations in this operator, an individual is selected as the parent. A sub-branch of the parental relationship is deleted randomly. Then, another sub-branch is randomly produced and replaced (Fig. 1).

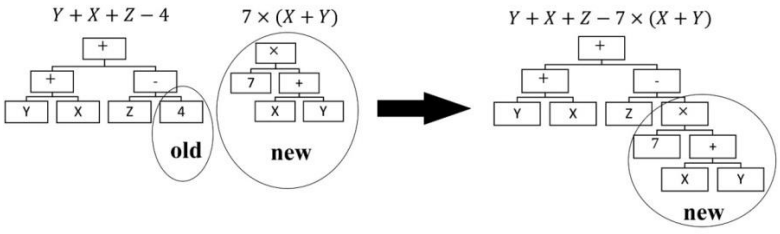

Figure 1. Applying mutation operator in GP

- **Crossover operator**

This operator is used to combine the genetic string of two individuals as the parent. In this combination, the production of a new generation is accomplished through the exchange of two random sub-branches of the parents with each other (Fig. 2).

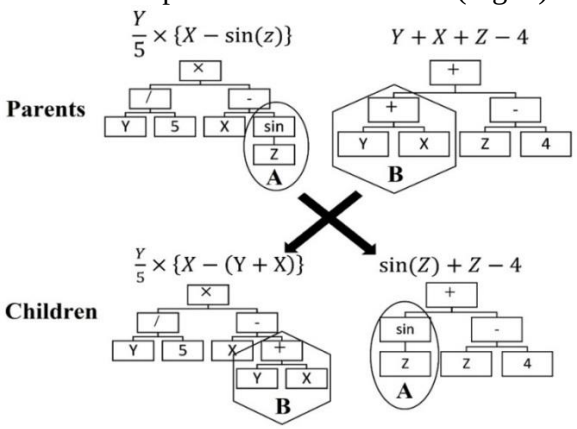

Figure 2. Applying Crossover operator in GP

Koza [20] explained the performance of GP in four steps. The first includes the production of a primary population from the random combination of the functions and terminals of the problem. Then, the accuracy of all of the equations produced in the previous step is checked. In the next step, by selecting the best available equations and using genetic operators, a new population is produced. In the fourth step, if the number of the specified generations is finished, the best equation is announced; otherwise, the process of problem solving is followed from the second step. The objective of GP is to find a very suitable equation in the space of the response. Production of the primary population is indeed a blind and random search for a response, which is directed by the GP process. To prevent the production of long and inapplicable equations, the dimensions of the tree equations should be limited.

3. DEVELOPING DAMAGE AND PLASTICITY CONSTANTS OF CONCRETE

As mentioned, in addition to the constants which are calculable based on the mechanical properties of the materials, Voyiadjis and Taqieddin [14] model included seven constants of Q, w, h, $a^{\pm}$ and $b^{\pm}$ which have no clear experimental definition (for more details, refer to Moradi et al. [18]). These constants were divided into two categories: compression (Q, w, a^{-} and b^{-}) and tension (h, a^{+} and b^{+}) and computed in part I of this work using genetic algorithm optimization [18]. In this study, the GP method is used to extract equations for predicting the damage and plasticity constants of concrete. GP needs some input and output data to extract the mathematic relationship; accordingly, the results of part I of this work including the results of these constants for 44 experimental samples were used [18]. Since the factors affecting the damage and plasticity constants were unknown and indefinite, different input variables were used to calculate an appropriate equation. The considered input variables can be directly calculated from the uniaxial tensile and compressive stress-

strain curve. It should be noted that although GP is a powerful statistical tool for making equations, any smart guess of the response form or at least the combination of the variables can help achieve an optimal response with less computational costs [24].

3.1 GP code setting

To model the GP, a set of codes provided by Silva and Almeida [24] was used with some modifications. The absolute error value in the GP code was defined as the objective function; in other words, the value of the objective function in any equation in the GP computational operation was the absolute sum of the difference between the optimization results and those obtained from the equation for all the samples. Any equation with more absolute error would have more inappropriate results. The probability of selecting the parents for the use of the operators was considered with regard to the ranking of their accuracy in estimating the problem [25]. The mathematical operators including $\times, +, -, /$, power, square and sinus together with some random and constant numbers were used. 1000 individuals and 300 generations were used to calculate the equations. The GP codes were executed for various groups of the input values; consequently, in addition to determining the effective inputs, the access to the most accurate equation became possible. Results of these calculations are represented in the following section. Similar to the investigations conducted in part I of this work, the constants of Q, W, a^- and b^- and the constants of h, a^+ *and* b^+ were determined based on the uniaxial compressive test and the uniaxial tensile test, respectively [18].

3.2 Equations of damage and plasticity constants based on uniaxial compressive test

Thirty experimental samples of uniaxial compressive collected from the relevant literature are examined in this section [2, 3, 5, 6, 26-31]. Values of the compressive plasticity and damage constants were considered for modeling these tests based on the calculations by Moradi et al. [18]. Table (1) shows these constants along with the primary values used in this study. In this table, E, f_0, f_c, f_u, ε_c and ε_u indicate the elasticity modulus, initial stress of the non-linear behavior, compressive strength, ultimate compressive stress, strain at compressive strength and ultimate compressive strain, respectively. Besides, A_T is the absolute value of the area under the compressive stress-strain diagram.

Beside the values presented in Table (1), some combinations of these values were also considered as the input data. These values included the approximate effective area under the stress-strain diagram (α_T), the approximate area under the strain-hardening diagram (α_c) and the equivalent slope of the descending branch (S). Eq. (1), (2) and (3), could be used for calculation of α_c, α_T and S respectively. In these equations, the symmetrical slope of the descending branch was considered as the S variable in order to have a positive value. Further, the Q/W ratio that is a variable affecting Y_0^- (the initial conjugate forces of the compressive damage threshold) was also considered as Q_w (Eq.4) [18]. This variable was used in the proposed equation for a^-. The value of this factor in developing the equations was considered as the value obtained from optimization, while for the ultimate calculations and error control, Q_w was determined using the proposed equations of Q and W and applied in the proposed equation for a^-.

$$\alpha_c = \frac{f_0^2}{2E} + \frac{f_0 + f_c}{2}\left(\varepsilon_c - \frac{f_0}{E}\right) \quad (1)$$

$$\alpha_T = \alpha_c + (\varepsilon_u - \varepsilon_c)\frac{f_u - f_c}{2} \quad (2)$$

$$S = -\frac{f_u - f_c}{\varepsilon_u - \varepsilon_c} \quad (3)$$

$$Q_w = \frac{Q}{W} \quad (4)$$

Fig. 3(A), 3(B), 4 and 5 show the tree relationships of the GP output for the constants of Q, b^-, W and a^-, respectively. Investigation of the proposed equations of GP for b^- showed that eliminating the size effect could lead to much more accurate equations; thus, in order to eliminate the size effect, the input and output data were divided by their maximum values to have a value between zero and one, which can be observed in the obtained equations. The mathematical form of the equations of Q, W, b^- and a^- can be observed without any modification in Eq. (5-8). These equations can be expresses with minimum simplifications in the form of Eq. (9-12).

Table 1: Primary values based on uniaxial compressive test

Specimen	**Primary values (inputs)**							**Compressive constants values calculated based on optimization [18]**			
	E (MPa)	f_0 (MPa)	f_c (MPa)	f_u (MPa)	ε_c	ε_u	A_T (MPa)	W	Q	b^-	a^-
C1 (Wee et al. [5])	49051	58.7	122.6	59.5	0.00273	0.00326	0.24541	756	129.6	6.97	5.22
C2 (Wee et al. [5])	45658	58.0	105.7	27.3	0.00256	0.00570	0.31255	688	103.4	2.25	4.33
C3 (Wee et al. [5])	42871	50.6	85.8	20.7	0.00228	0.00575	0.26382	726	81.8	2.01	6.00
C4 (Wee et al. [5])	41070	23.7	66.6	20.7	0.00230	0.00574	0.23208	1261	79.6	1.97	6.01
C5 (Wee et al. [5])	36463	29.4	46.7	15.3	0.00198	0.00633	0.17883	867	37.9	1.58	9.94
C6 (Wee et al. [5])	28412	16.3	30.9	15.6	0.00217	0.00582	0.13371	881	28.0	1.31	13.39
C7 (Li and Ren [26])	38808	15.2	51.2	19.4	0.00191	0.00389	0.13123	1941	70.8	2.13	9.47
C8 (Karsan and Jirsa [2])	31000	10.9	27.6	15.5	0.00211	0.00500	0.10720	1366	29.3	1.11	18.11
C9 (Ali et al. [27])	13820	10.0	16.7	9.4	0.00177	0.00350	0.04242	763	10.5	1.78	29.72
C10 (Ali et al. [27])	19980	12.7	25.3	16.9	0.00196	0.00348	0.06237	969	21.4	1.79	18.58
C11 (Ali et al. [27])	23530	9.0	27.7	22.5	0.00199	0.00339	0.07261	1998	28.7	1.45	14.75
C12 (Ali et al. [27])	33980	9.1	32.0	28.3	0.00200	0.00336	0.08498	1902	35.3	1.04	15.04
C13 (Ali et al. [27])	44550	10.0	43.5	26.3	0.00200	0.00301	0.10321	1957	52.7	1.06	10.26
C14 (Kupfer [3])	30072	13.2	32.1	27.8	0.00223	0.00305	0.07561	975	28.6	1.31	13.58
C15 (Dahl [28])	18050	9.7	22.0	13.7	0.00270	0.00600	0.10444	821	17.9	1.07	16.67
C16 (Dahl [28])	25493	10.2	32.1	13.7	0.00273	0.00598	0.14350	883	31.3	1.37	11.23
C17 (Dahl [28])	33574	11.0	50.1	20.1	0.00273	0.00500	0.16985	1127	59.9	2.05	7.39
C18 (Dahl [28])	33990	18.0	65.0	7.8	0.00260	0.00598	0.19179	1110	78.6	2.77	6.96
C19 (Dahl [28])	40595	39.2	93.5	5.2	0.00262	0.00450	0.20145	880	103.5	5.51	6.29
C20 (Dahl [28])	41361	84.2	105.4	4.1	0.00270	0.00455	0.20949	175	76.5	3.90	9.46
C21 (Carreira and Chu [29])	27177	36.5	46.4	45.7	0.00217	0.00238	0.06926	238	27.9	2.14	10.98
C22 (Carreira and Chu [29])	23115	22.0	34.9	33.1	0.00220	0.00273	0.06631	558	25.3	1.91	12.17
C23 (Carreira and Chu [29])	18748	7.9	20.0	15.1	0.00194	0.00412	0.06551	3045	18.1	1.17	21.68
C24 (Carreira and Chu [29])	26033	23.8	73.6	16.3	0.00358	0.00597	0.25451	698	82.0	4.09	4.47
C25 (Carreira and Chu [29])	20974	19.5	50.7	15.2	0.00297	0.00582	0.17627	1070	59.1	2.70	7.14
C26 (Carreira and Chu [29])	17222	17.4	40.5	13.3	0.00288	0.00582	0.14321	965	42.0	2.42	8.97
C27 (Carreira and Chu [29])	10636	6.7	20.7	13.6	0.00267	0.00583	0.08775	2291	18.7	1.67	13.92
C28 (Muguruma and	38105	33.3	65.6	32.3	0.00377	0.02183	1.06275	387	68.1	0.91	3.83

Watanabe [30])											
C29 (Sinha et al. [31])	20197	9.6	26.0	14.5	0.00264	0.00655	0.13104	958	25.5	1.30	12.82
C30 (Ren et al. [6])	39772	41.0	65.0	15.9	0.00209	0.00497	0.16895	682	56.6	1.91	9.97

$$Q = f_c - f_0 + \frac{f_c}{0.69395 \times 0.2465 \times 10} - 0.16174^{-1} \tag{5}$$

$$W = \frac{Q - f_0}{\alpha_T} + \frac{Q}{\alpha_c} + (100 - f_c\ - (f_0 + f_c)\ ) - f_c + (0.23481Q)^{\frac{\sin(\frac{\alpha_T}{\alpha_c})}{\alpha_c f_0}} \tag{6}$$

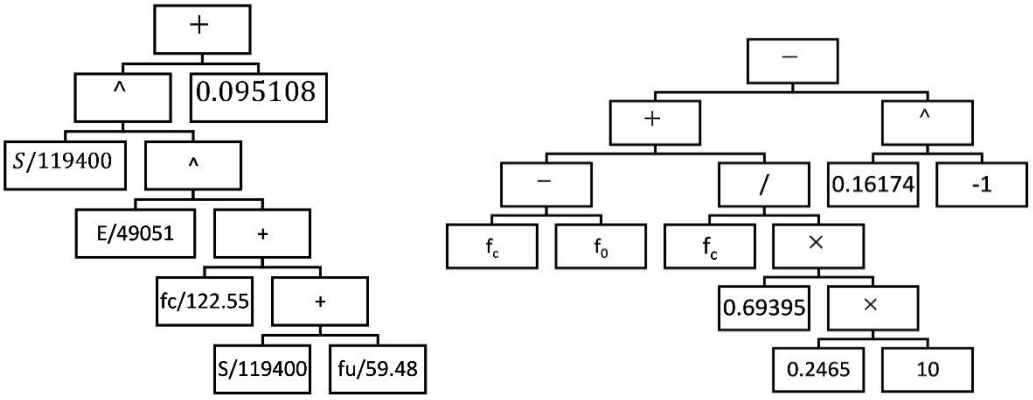

(a) Q (b) b^-

Figure 3. Tree diagram of GP output results

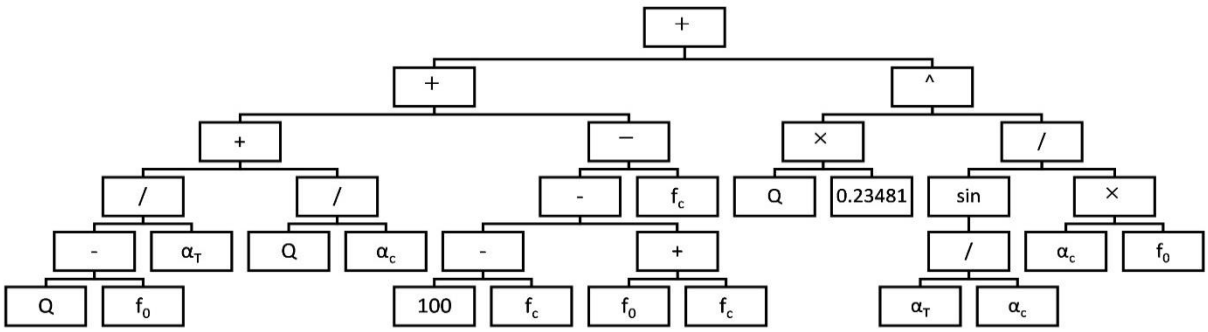

Figure 4. Tree diagram of GP output result for W

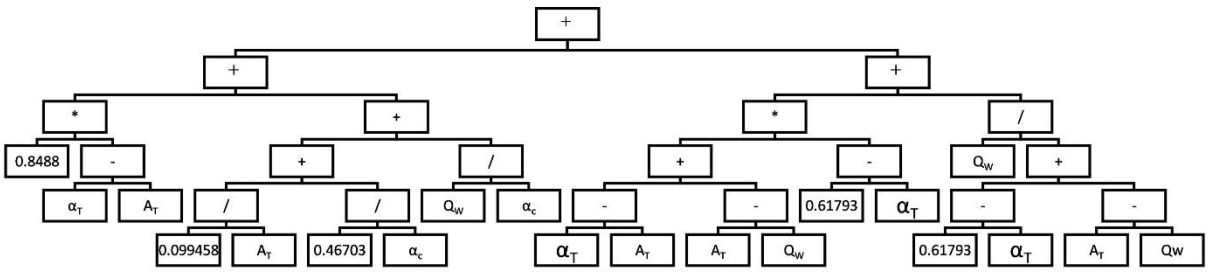

Figure 5. Tree diagram of GP output result for a^-

$$a^- = 0.8488(\alpha_T - A_T) + \frac{0.099458}{A_T} + \frac{0.46703}{\alpha_c} + \frac{Q_W}{\alpha_c} + ((\alpha_T - A_T) + (A_T - Q_W))(0.61793\alpha_T) + \left(\frac{Q_W}{0.61793 - \alpha_T + A_T - Q_W}\right) \quad (7)$$

$$\frac{b^-}{6.968} = \left(\frac{S}{119400}\right)^{\left(\frac{E}{49051}\right)^{\left(\frac{f_c}{122.55} + \frac{S}{119400} + \frac{f_u}{59.48}\right)}} + 0.095108 \quad (8)$$

$$Q = 1.58459 f_c - f_0 - 6.1828 \quad (9)$$

$$W = \frac{Q - f_0}{\alpha_T} + \frac{Q}{\alpha_c} + 100 - f_0 - 3f_c + (0.23481Q)^{\frac{\sin(\frac{\alpha_T}{\alpha_c})}{\alpha_c f_0}} \quad (10)$$

$$a^- = 0.8488(\alpha_T - A_T) + \frac{0.09946}{A_T} + \frac{Q_W + 0.467}{\alpha_c} + (\alpha_T - Q_W)(0.6179\alpha_T) + \left(\frac{Q_W}{0.6179 - \alpha_T + A_T - Q_W}\right) \quad (11)$$

$$b^- = 6.968 * \left(\frac{S}{119400}\right)^{\left(\frac{E}{49051}\right)^{\left(\frac{f_c}{122.55} + \frac{S}{119400} + \frac{f_u}{59.48}\right)}} + 0.66271 \quad (12)$$

One of the variables in the equation presented for a^- is the area under the stress-strain diagram (A_T) (Eq.11). It may be difficult to determine the area under the diagram in some cases. In Appendix (A), an equation without this variable is introduced for a^-; however, the error of this equation is slightly more than Eq. (11).

In Table (2), the statistical indices of the proposed equations are investigated. As can be seen, the proposed equations predict the values of the damage and plasticity constants with maximum mean error of 11%. Despite good accuracy of each equation, since none of these constants can be applied individually, it is necessary to test their accuracy in modeling. Thus, Voyiadjis and Taqieddin [14] model was implemented in MATLAB for an element under the uniaxial loading. all the samples were modeled using the constants obtained from the proposed equations. To compare the error of this modeling, an objective function similar to the one in part I of this work was used (Eq.13) [18]. The obtained results associated with the constants calculated for each sample are collected in Table 3 and compared with the results of optimization. The objective function is absolute value of the mean relative error in the whole stress-strain diagram. The mean of the objective function can be a good index for evaluating the accuracy of these constants. This value was 0.0407 for the samples which used the optimized constants; in other words, the mean error in the prediction of the stress-strain diagram was 4%. This error value will never be lower because the constants are obtained using optimization; in fact, this error value is the internal error of the constitutive model. The mean value of the objective function for the results of modeling with the constants obtained from the proposed equations was 0.0759; therefore, it can be said that, using the proposed equations, the uniaxial compressive stress-strain diagram can be determined with the error of 3.52% relative to the optimization results. According to the statistical nature of the experimental results of concrete, this error is acceptable. In Fig. 6 and 7, the uniaxial compressive stress-strain diagrams obtained from modeling based on the constants presented in this study were compared with their corresponding experimental

results. In these figures, a good agreement is generally found between the experimental and modeling results; however, there is a slight error in the prediction of the results of the high-strength concrete specimens.

Table 2: Statistical investigation of proposed equations

Equation	R^2	SAE[a,b]	MAPE[c]
Equation presented for Q [Eq. (9)]	0.991	55.7	4.2
Equation presented for W [Eq. (10)]	0.934	3408.7	10.9
Equation presented for a^- [Eq. (11)]	0.955	24.2	7.9
Equation presented for b^- [Eq. (12)]	0.915	7.1	10.1

[a] Sum of Absolute Errors= $\sum \left| f_{sp_{\text{predict}}} - f_{sp_{\text{exp}}} \right|$

[b] Objective function in GP

[c] Mean Absolute Percentage Error=$mean \left| \frac{f_{sp_{\text{predict}}} - f_{sp_{\text{exp}}}}{f_{sp_{\text{predict}}}} \right|$

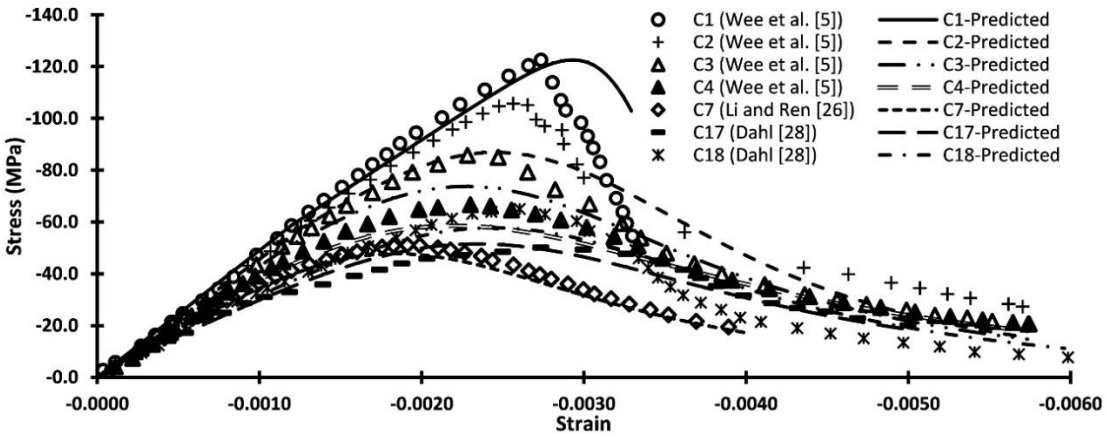

(a) Part I

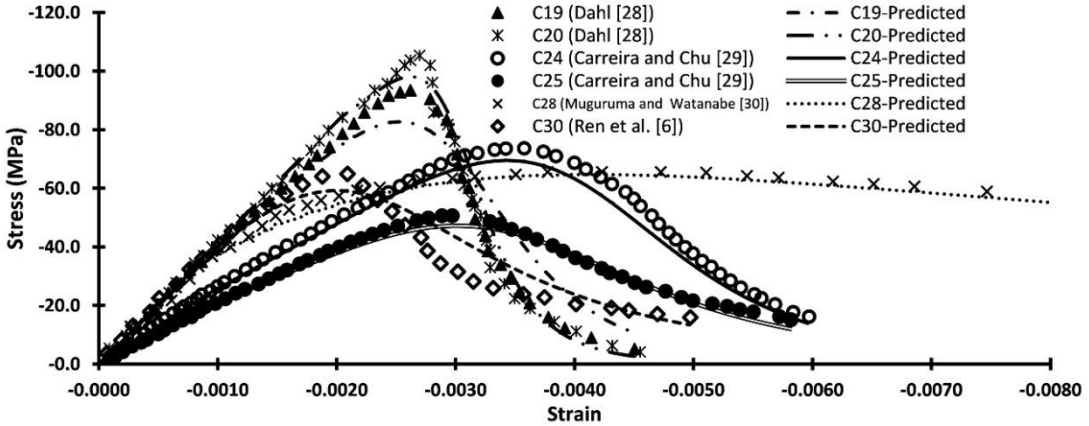

(b) Part II

Figure 6. Comparison of stress-strain diagrams of uniaxial compressive tests obtained from experimental and modeling results of samples with compressive resistance of more than 50 MPa

$$F_{objective} = \frac{1}{n}\sum_{i=1}^{n}\left|\frac{\sigma(\varepsilon_i, calculation) - \sigma(\varepsilon_i, experimental)}{\sigma(\varepsilon_i, experimental)}\right| \quad (13)$$

Table 3: Investigating accuracy of modeling the uniaxial compressive test based on constants obtained from the proposed equations

Specimen	Values of constants calculated based on optimization [18]					Values of constants calculated based on the proposed equations (GP)				
	Q	W	b^-	a^-	$F_{objective}$	Q	W	b^-	a^-	$F_{objective}$
C1 (Wee et al. [5])	129.6	756.2	6.97	5.22	0.0414	129.3	785.0	7.63	4.32	0.1502
C2 (Wee et al. [5])	103.4	687.6	2.25	4.33	0.0676	103.4	621.1	2.38	5.08	0.1121
C3 (Wee et al. [5])	81.8	725.8	2.01	6.00	0.0627	79.2	679.3	2.11	6.15	0.0717
C4 (Wee et al. [5])	79.6	1261.5	1.97	6.01	0.0496	75.7	1090.7	1.78	6.86	0.0743
C5 (Wee et al. [5])	37.9	867.0	1.58	9.94	0.0619	38.5	688.8	1.38	9.90	0.1132
C6 (Wee et al. [5])	28.0	881.5	1.31	13.39	0.0407	26.4	771.7	1.25	12.59	0.0869
C7 (Li and Ren [26])	70.8	1940.8	2.13	9.47	0.0157	59.7	1598.6	2.02	10.25	0.0533
C8 (Karsan and Jirsa [2])	29.3	1365.8	1.11	18.11	0.0252	26.7	1159.2	1.16	14.64	0.0819
C9 (Ali et al. [27])	10.5	763.4	1.78	29.72	0.0314	10.3	787.5	1.43	29.76	0.0597
C10 (Ali et al. [27])	21.4	968.9	1.79	18.58	0.0569	21.2	1036.1	1.71	18.31	0.0605
C11 (Ali et al. [27])	28.7	1997.7	1.45	14.75	0.0162	28.7	1956.7	1.45	16.84	0.0477
C12 (Ali et al. [27])	35.3	1901.5	1.04	15.04	0.0164	35.4	1890.3	1.06	14.38	0.0204
C13 (Ali et al. [27])	52.7	1956.6	1.06	10.26	0.0422	52.8	1912.8	1.84	11.17	0.0944
C14 (Kupfer [3])	28.6	975.0	1.31	13.58	0.0286	31.6	1145.5	1.48	12.74	0.0538
C15 (Dahl [28])	17.9	820.9	1.07	16.67	0.0171	19.1	791.1	1.23	14.29	0.0576
C16 (Dahl [28])	31.3	883.4	1.37	11.23	0.0404	34.4	1019.0	1.48	10.50	0.0500
C17 (Dahl [28])	59.9	1127.1	2.05	7.39	0.0498	62.3	1260.7	2.09	7.50	0.0587
C18 (Dahl [28])	78.6	1109.5	2.77	6.96	0.0714	78.8	1082.9	2.29	6.64	0.1768
C19 (Dahl [28])	103.5	880.5	5.51	6.29	0.0564	102.7	880.4	3.99	5.31	0.2018
C20 (Dahl [28])	76.5	175.4	3.90	9.46	0.0566	76.6	185.9	4.42	8.74	0.0885
C21 (Carreira and Chu [29])	27.9	238.0	2.14	10.98	0.0274	30.8	354.1	1.88	10.99	0.0320
C22 (Carreira and Chu [29])	25.3	557.9	1.91	12.17	0.0293	27.2	680.8	1.78	12.58	0.0359
C23 (Carreira and Chu [29])	18.1	3044.5	1.17	21.68	0.0263	17.5	2715.7	1.17	22.28	0.0307
C24 (Carreira and Chu [29])	82.0	698.4	4.09	4.47	0.0305	86.7	775.9	3.75	4.71	0.0633
C25 (Carreira and Chu [29])	59.1	1070.4	2.70	7.14	0.0361	54.6	877.6	2.82	7.22	0.0421
C26 (Carreira and Chu [29])	42.0	965.5	2.42	8.97	0.0385	40.7	842.7	2.52	8.97	0.0410
C27 (Carreira and Chu [29])	18.7	2290.8	1.67	13.92	0.0199	19.8	2808.2	1.51	16.89	0.0899
C28 (Muguruma and Watanabe [30])	68.1	387.0	0.91	3.83	0.0454	64.4	346.9	0.96	3.94	0.0768
C29 (Sinha et al. [31])	25.5	957.5	1.30	12.82	0.0278	25.4	986.1	1.28	12.86	0.0288
C30 (Ren et al. [6])	56.6	682.1	1.91	9.97	0.0913	55.8	663.8	2.07	7.97	0.1230

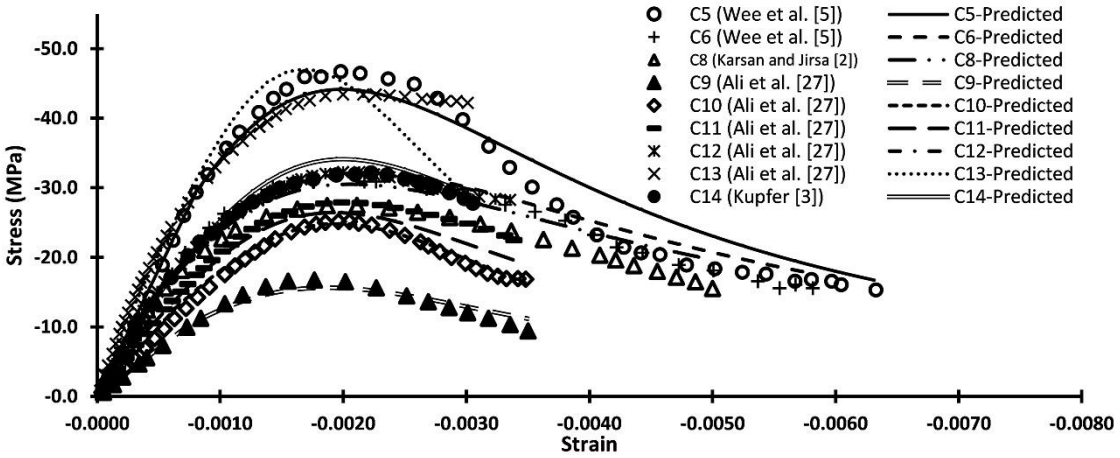

(a) Part I

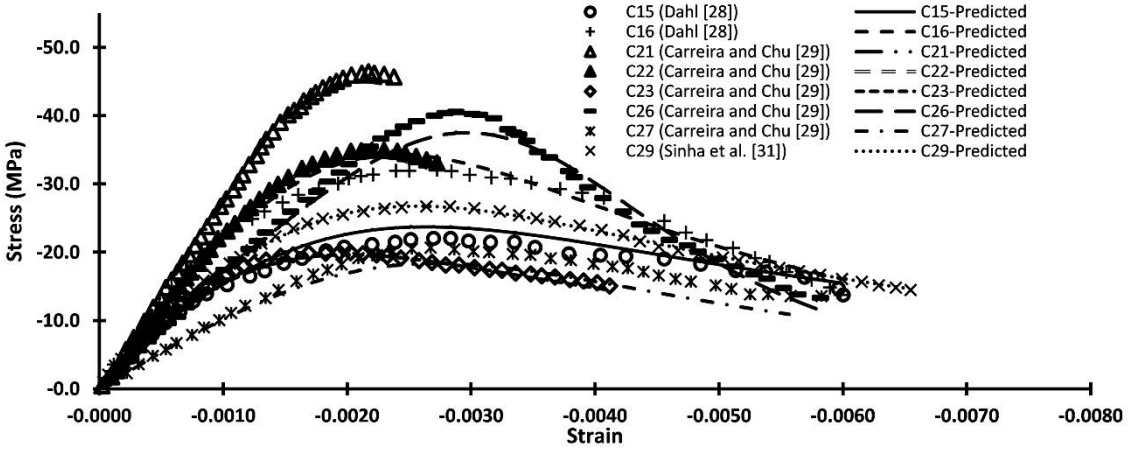

(b) Part II

Figure 7. Comparison of stress-strain diagrams of uniaxial compressive tests obtained from experimental and modeling results of samples with compressive resistance of less than 50 MPa

3.3 Equations of damage and plasticity constants based on uniaxial tension test

Fourteen experimental uniaxial tension samples collected from the relevant literature are investigated in this section (Table 4) [3, 4, 6, 7, 32-37]. The value of the damage and plasticity constants affecting the tension (h, a^+ and b^+) were considered according to the calculations in part I of this work [18]. These constants as well as the primary values used in this study are shown in Table (4). In this table, f_t, f_{tu}, ε_{tu} *and* A_{TT} indicate the tensile strength, ultimate tension stress, ultimate tensile strain and the area under the tensile strain-stress diagram, respectively. These values were directly calculated based on the tensile strain-stress diagram. In addition to the values introduced in Table (4), the equivalent slope of the descending branch of the uniaxial tensile stress-strain diagram (S_t) was also considered as an input value (Eq.14).

$$S_t = \frac{f_{tu} - f_t}{\varepsilon_{tu} - \varepsilon_t} \tag{14}$$

Table 4: Primary values based on uniaxial tensile test

Specimen	Primary values (inputs)						Tensile constants values calculated based on optimization [18]		
	E (MPa)	f_c (MPa)	f_t (MPa)	f_{tu} (MPa)	ε_{tu}	A_{TT} (MPa)	h	b^+	a^+
T1 (Meng et al. [32])	16400	37.1	2.03	0.064	0.005001	0.00164	13127	1.210	2400
T2 (Meng et al. [32])	24522	67.6	3.70	0.123	0.004988	0.00287	3877	1.126	1920
T3 (Meng et al. [32])	38318	83.0	4.60	0.045	0.004965	0.00290	2964	1.416	941
T4 (Huo et al. [7])	45493	46.8	4.49	0.385	0.001988	0.00146	4404	0.849	6254
T5 (Reinhardt et al. [4])	30288	47.1	3.44	0.194	0.003977	0.00325	3643	1.178	975
T6 (Reinhardt et al. [4])	16576	48.6	2.56	0.045	0.003973	0.00214	3214	1.455	1177
T7 (Yan and Lin [33])	28265	65.0	2.22	0.202	0.000367	0.00031	4181	1.205	8661
T8 (Akita et al. [34])	39370	33.4	2.88	0.121	0.000623	0.00059	3536	1.006	5403
T9 (Akita et al. [34])	38291	29.7	3.25	0.783	0.000924	0.00148	8573	1.043	1714
T10 (Gopalaratnam and Shah [35])	31000	46.8	3.53	0.496	0.000437	0.00067	1136	1.096	5705
T11 (Zhang [36])	34403	47.2	3.40	0.103	0.000256	0.00034	3175	1.848	8258
T12 (Li et al. [37])	20347	46.8	4.01	0.827	0.001211	0.00236	4969	1.116	950
T13 (Ren et al. [6])	39772	65.0	2.59	0.784	0.000752	0.00096	4015	0.999	2335
T14 (Kupfer et al. [3])	33072	32.1	2.91	2.892	0.000096	0.00014	3669	1.018	19379

Fig. 8 shows output tree relations of GP for h, a^+ and b^+constants. similar Eq. (8), in order to eliminate the size effect in the equation for b^+, the output and input data were divided by their maximum values to have a value between zero and one, which could be observed in the obtained equation. Eq. (15-17) show the mathematical forms of the equations of h, a^+, $and\ b^+$, respectively, without any change. These equations can be represented with minimum simplification based on Eq. (18-20).

$$H = \frac{\left(\frac{1}{0.11818}\right)^{\left(\frac{\varepsilon_{tu}}{A_{TT}}\right)} - 1(100+1)}{f_{tu}} - \left(\frac{f_c - \{-1\} + 10}{\frac{\varepsilon_{tu}}{A_{TT}} - \{0.51684 - 0.11818\}} - \frac{f_{tu} + 100}{0.18514 \times 0.11818}\right) \tag{15}$$

$$a^+ = \frac{f_t + b^+ + 0.40597}{A_{TT}} - \frac{\frac{b^+}{\varepsilon_{tu}}}{0.93848} + 100 - 10 f_c b^+ - \frac{0.82897 f_c}{f_{tu} - 0.39662} \tag{16}$$

$$b^+ = 1.8479 \times 0.43073 \left\{ \left([0.65001]^{\left(\frac{S}{20918} \times \frac{A_{TT}}{0.00325}\right)} \right)^{\left(\frac{A_{TT}}{0.00325}\right)/\left(\frac{f_{tu}}{2.891}\right)} \times \left[\frac{E}{45493}\right]^{\left(\frac{E}{45492}\right)^{\left(\frac{f_t}{4.596}\right)}} \times \left[\frac{f_{tu}}{2.891}\right]^{\left(\frac{S}{20918} \times \frac{S}{20918}\right)} \right\} \tag{17}$$

$$H = \frac{8.4617^{\left(\frac{\varepsilon_{tu}}{A_{TT}}\right)} - 110}{f_{tu}} - \left(\frac{f_c + 11}{\frac{\varepsilon_{tu}}{A_{TT}} - 0.635} - \frac{f_{tu} + 100}{0.02188}\right) \tag{18}$$

$$a^+ = \frac{f_t + b^+ + 0.406}{A_{TT}} - \frac{b^+}{0.938\varepsilon_{tu}} + 100 - 10 f_c b^+ - \frac{0.829 f_c}{f_{tu} - 0.397} \tag{19}$$

$$b^+ = 1.8479 \times 0.4307^{\left\{\left([0.65]^{\left(\frac{S \times A_{TT}}{67.98}\right)}\right)^{900 \times \left(\frac{A_{TT}}{f_{tu}}\right)} \times \left[\frac{E}{45493}\right]^{\left(\frac{E}{45492}\right)^{\left(\frac{f_t}{4.596}\right)}} \times \left[\frac{f_{tu}}{2.891}\right]^{\left(\frac{S}{119400}\right)^2}\right\}} \tag{20}$$

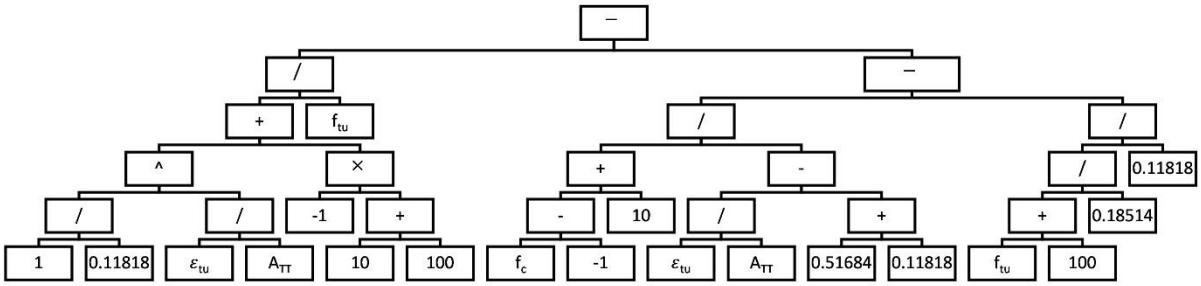

(a) h

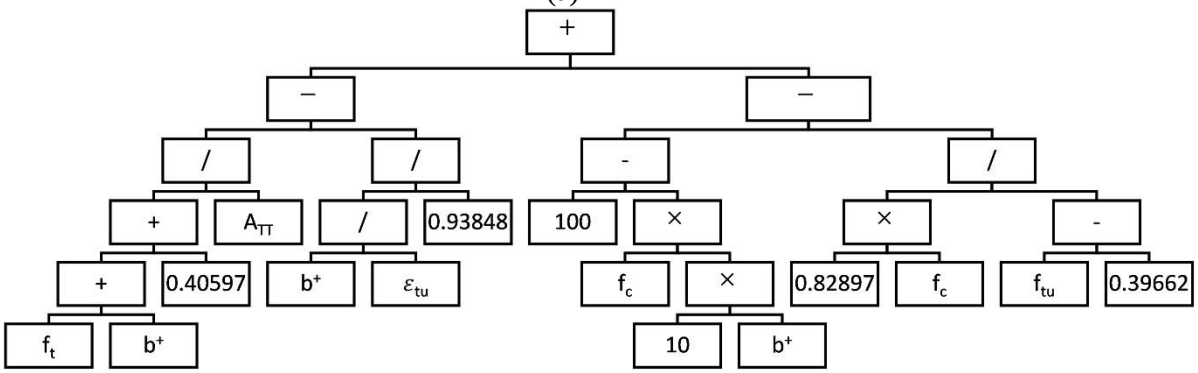

(b) a^-

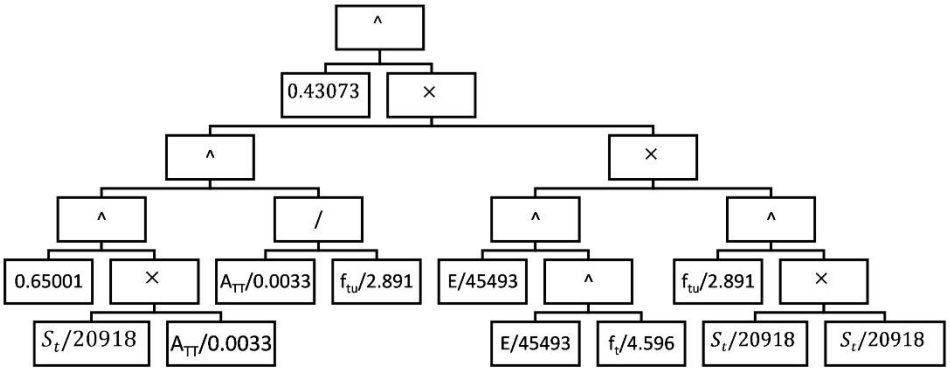

(c) b^-

Figure 8. Tree diagram of GP output results

In Table (5), the statistical indices of the proposed equations are studied. These indices confirm the appropriate equation development of the constants; however, as previously mentioned, the error of the equations is revealed in modeling. In Table (6), the results of modeling along with the constants calculated for each sample were collected and compared with the optimization results.

Table 5: Statistical investigation of proposed equations (tensile plasticity and damage constants)

Equation	R^2	SAE	MAPE
Equation presented for h [Eq. (18)]	0.998	1439.3	1439.3
Equation presented for a^+ [Eq. (19)]	0.985	4473.0	4473.0
Equation presented for b^+ [Eq. (20)]	0.922	0.76	0.76

According to the results in Table (6), the mean value of the objective function was 0.098 for the samples using optimization constants. but the mean value of the objective function for the results of modeling with the constants obtained from the proposed equations was 0.125. thus, the proposed equations can determine the uniaxial tensile stress-strain diagram with the error of 2.7% compared to the optimization results. It must be mentioned that the remaining error is the internal error of the model that has not been removed even by optimization. The value of this error for the samples with higher ultimate strain was larger. Regarding the statistical nature of the experimental results of the concrete as well as the significant complexity of the uniaxial tensile test, this error could be acceptable.

Table 6: Investigating accuracy of modeling the uniaxial tensile test based on constants obtained from the proposed equations

Specimen	Values of constants calculated based on optimization [18]				Values of constants calculated based on the proposed equations (GP)			
	h	b^+	a^+	$F_{objective}$	h	b^+	a^+	$F_{objective}$
T1 (Meng et al. [32])	13127	1.210	2400	0.132	13159	1.241	1704	0.263
T2 (Meng et al. [32])	3877	1.126	1920	0.093	3943	1.196	1086	0.122
T3 (Meng et al. [32])	2964	1.416	941	0.169	2891	1.421	1027	0.190
T4 (Huo et al. [7])	4404	0.849	6254	0.152	4270	0.856	6404	0.161
T5 (Reinhardt et al. [4])	3643	1.178	975	0.089	3982	1.145	980	0.107
T6 (Reinhardt et al. [4])	3214	1.455	1177	0.086	3234	1.340	1214	0.147
T7 (Yan and Lin [33])	4181	1.205	8661	0.072	3964	1.215	8586	0.072
T8 (Akita et al. [34])	3536	1.006	5403	0.127	3642	1.054	5409	0.133
T9 (Akita et al. [34])	8573	1.043	1714	0.074	8477	0.945	1774	0.104
T10 (Gopalaratnam and Shah [35])	1136	1.096	5705	0.088	1121	1.228	3855	0.132
T11 (Zhang [36])	3175	1.848	8258	0.083	3057	1.810	8334	0.085
T12 (Li et al. [37])	4969	1.116	950	0.073	4954	1.140	827	0.096
T13 (Ren et al. [6])	4015	0.999	2335	0.090	3972	0.907	2169	0.098
T14 (Kupfer et al. [3])	3669	1.018	19379	0.042	3832	0.966	19688	0.042

The uniaxial tensile stress-strain diagrams resulted from modeling based on the proposed constants in this study were compared with their corresponding experimental results in Fig.

9. In these figures, a good agreement is observed between the experimental and modeling results.

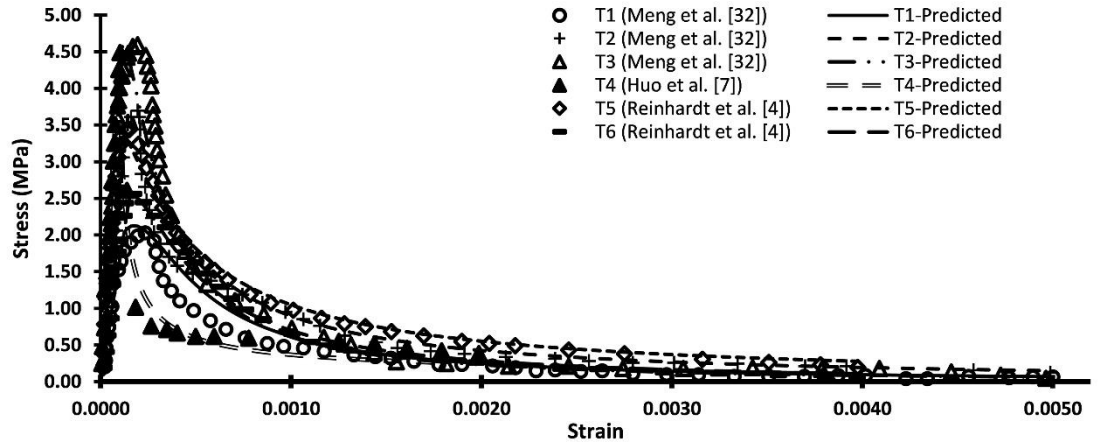

(a) T1-T6

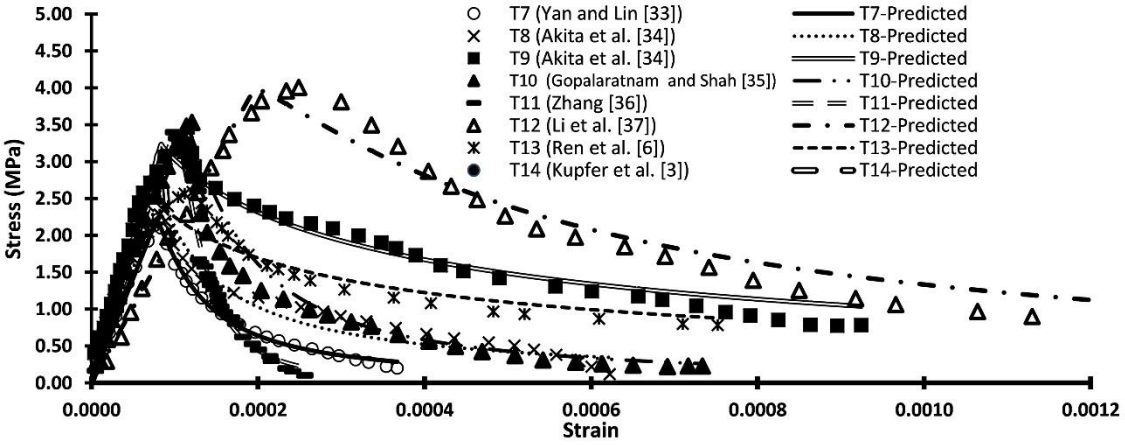

(b) T7-T13

Figure 9. Comparison of stress-strain diagrams of uniaxial tensile test obtained from modeling and experimental results

4. INVESTIGATING THE CONSTANTS OBTAINED FROM THE PROPOSED EQUATIONS FOR EXPERIMENTAL DATA AND CYCLIC AND BIAXIAL TESTS

4.1. Experimental data

One of the things based on which the proposed equations should be assessed is the data that do not contribute to the process of equation development (experimental data). Although this issue is ignored in many of the similar studies, it is one of the most important and valuable criteria for evaluating the results. For this purpose, six uniaxial compressive tests and one uniaxial tensile test were extracted from the relevant literature [2, 38]; then, based on the proposed

equations, their related constants were determined (Tables 7 and 8). Using these constants, the uniaxial stress-strain diagram was determined through simulated in MATLAB environment (Fig. 10). As seen in Fig. 10, there was a good agreement between the experimental and modeling results. The strength of the samples in the modeling is determined conservatively less than the real value, which is desirable in civil engineering problems.

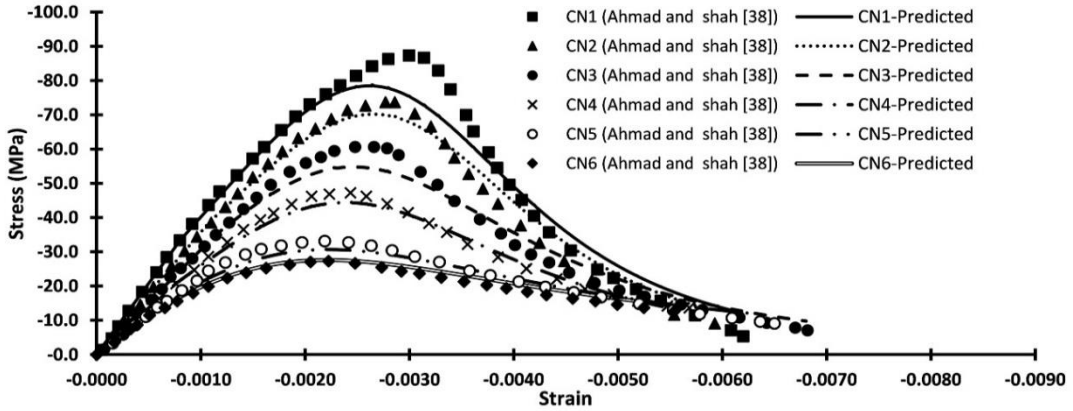

(a) CN1-CN6

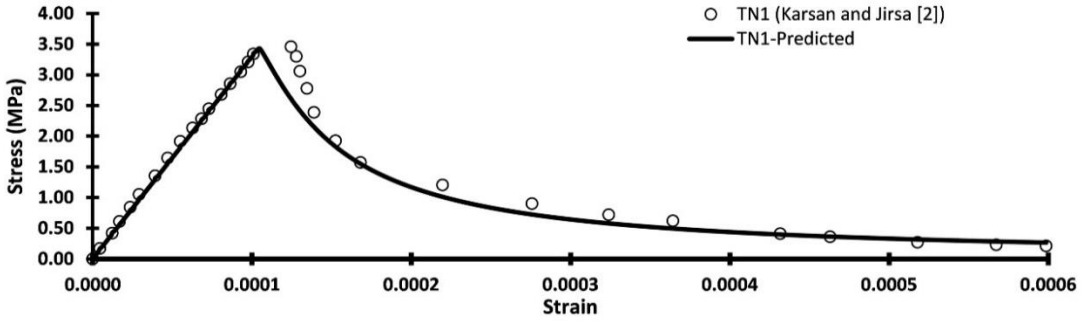

(b) TN1

Figure 10. Comparison of stress-strain diagrams obtained from modeling and experimental results (experimental data)

Table 7: Primary values and damage and plasticity constants of experimental-data based on uniaxial compressive test

Specimen [38]	**Primary values (inputs)**						**Values of constants calculated based on the proposed equations (GP)**					$F_{objective}$
	E (MPa)	f_0 (MPa)	f_c (MPa)	f_u (MPa)	ε_c	ε_u	A_T (MPa)	W	Q	b^-	a^-	
CN1	0.00620	41584	33.4	87.3	5.3	0.00300	0.27850	721	98.8	2.56	4.83	0.109
CN2	0.00593	35721	38.5	73.7	9.1	0.00286	0.23477	592	72.1	2.58	5.57	0.078
CN3	0.00682	30595	35.0	60.6	7.1	0.00248	0.21039	641	54.9	2.04	7.27	0.101
CN4	0.00568	27202	20.7	47.2	13.6	0.00243	0.16163	912	47.9	2.04	8.74	0.036
CN5	0.00650	23232	15.6	33.2	9.1	0.00219	0.13496	886	30.8	1.47	12.67	0.061
CN6	0.00554	22539	13.6	27.3	12.6	0.00222	0.10598	820	23.4	1.37	14.28	0.058

Table 8: Primary values and damage and plasticity constants of experimental-data based on uniaxial tensile test

Specimen	Primary values (inputs)						Values of constants calculated based on the proposed equations (GP)			F_{objec}
	E (MPa)	f_c (MPa)	f_t (MPa)	f_{tu} (MPa)	ε_{tu}	A_{TT} (MPa)	H	b^+	a^+	
TN1 (Karsan and Jirsa [2])	32903	27.6	3.46	0.2106	0.000124	0.0006326	3970	1.168	5778	0.0835

4.2. Cyclic tests

In the cyclic tests, the irreversible strains are clearly visible. Success in predicting these results is the evidence of success in modeling the plasticity of the materials. In this section, five compressive and tensile cyclic tests were modeled using the constants obtained from the proposed equations. These results were compared with the experimental results and the results presented by Moradi et al. [18] (Fig. 11 and 12). As shown in Fig. 11 and 12, modeling based on the proposed equations can predict the results of the cyclic tests with appropriate accuracy and success.

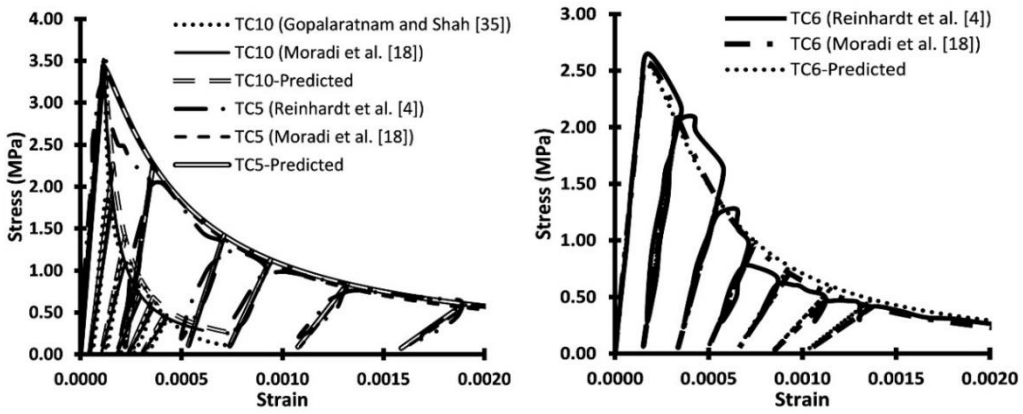

(a) TC5 and TC10 (b) TC6

Figure 11. Comparison of stress-strain diagrams of cyclic tensile tests obtained from experimental and modeling (TC5, TC6 and TC10 were made of materials similar to that of T5, T6 and T10, respectively)

4.3. Biaxial tests

In this section, to investigate the accuracy of the proposed equations in modeling, biaxial test was simulated in MATLAB environment for an element under the biaxial loading. As mentioned in part I of this work, the biaxial compressive tests need determination of the γ coefficient [18]. Due to the shortage of the corresponding uniaxial and biaxial experimental data required in the literature, it was impossible to develop an equation for this coefficient. Therefore, the values used in part I of this work were used for this purpose (the values of these coefficients for the biaxial sample corresponding to C7 and C14 were 0.538 and 0.421, respectively) [18].

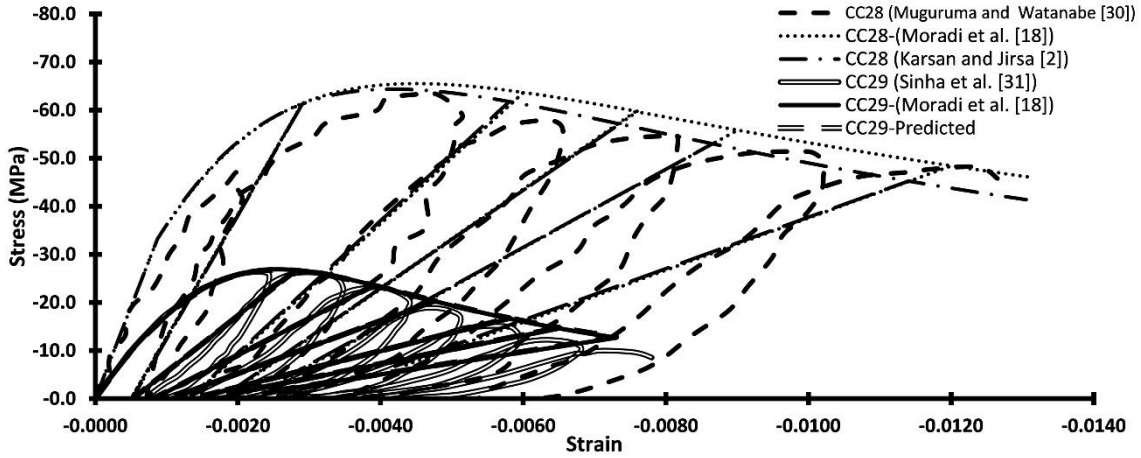

Figure 12. Comparison of stress-strain diagrams of cyclic compressive tests obtained from experimental and modeling (CC28 and CC29 were made of materials similar to that of C28 and C29, respectively)

In Fig. 13(A), the stress-strain diagram of the biaxial compressive test with different applied strain ratios for the concrete corresponding to C7 sample was compared with the modeling results. Further, the biaxial failure envelope for the concrete corresponding to the samples of T14 and C14 in Fig. 13(B) was compared with the modeling results. As seen in Fig. 13, modeling based on the constants obtained from the proposed equations may lead to the correct ultimate strength in the biaxial test; however, the consistency of the biaxial compressive diagrams is somehow problematic.

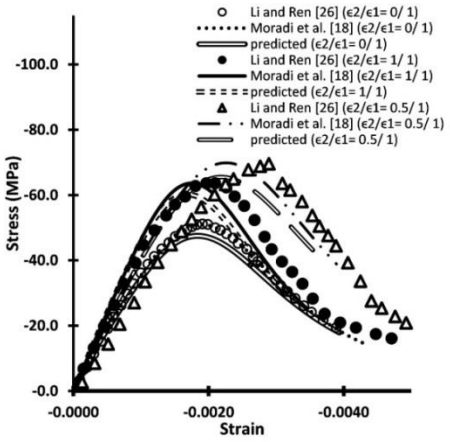

(a) Stress-strain diagram of biaxial compressive test for the concrete corresponding to specimens C7

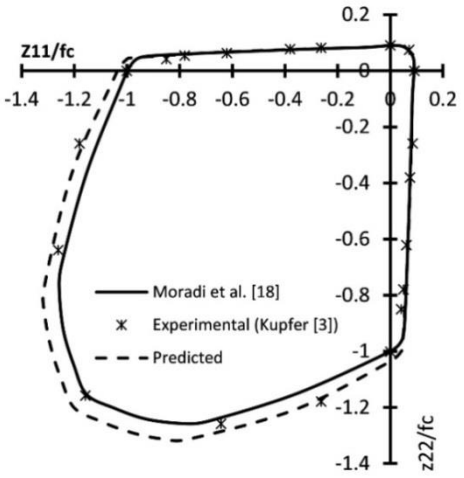

(b) Failure envelope for concrete corresponding to specimens T14 and C14

Figure 13. Comparison of experimental and modeling results, biaxial tests

5. SUMMARY AND CONCLUSION

In the present research, in order to determine the material constants of an elastic-plastic-damage model proposed for concrete, the results of 51 uniaxial compressive and tensile tests were used. Using the genetic programming method, direct equations were discovered for these constants. The results of the present study can be summarized as follows:

- Discovering the mathematical relations for the constants of the elastic-plastic-damage can be performed directly based on the uniaxial compressive and tensile tests. Modeling based on the constants derived from the discovered mathematical functions could predict the results of the uniaxial compressive and tensile tests with the mean errors of 3.6% and 2.7% respectively, compared to the optimization results. Furthermore, an appropriate response was also observed for the samples that were not used in equation discovery.
- Simulation of uniaxial, biaxial and cyclic tests showed reasonable accuracy by the elastic-plastic-damage model in which the constants obtained from the proposed equations were used. Therefore, it can be concluded that the concrete modeling is possible on this basis; however, for the use in more complicated constructions, these equations require further investigations.
- Using the proposed equations for normal-strength concretes leads to obtain appropriate responses. Despite relatively high error rate of these equations for high strength concrete, these equations can be used to determine the primary values of the damage and plasticity constants used in this strength range. It should be noted that the experimental results of the concrete have generally a highly dispersive statistical distribution. Since the method which was applied in the present study estimates less stress and resistance than the test amounts, it could be concluded that using the present method is a conservative way to cover the possible errors.

APPENDIX-A. EQUATION OF a^- WITHOUT VARIABLE OF A_T

In genetic programming for a^- constant, an equation without the variable of the area under the curve (A_T) was also calculated. The tree form of this equation and its simplified mathematical form are shown in Fig. 14 and Eq. (21), respectively. This equation has a higher error rate than Eq.(11) (Table 9); however, regarding the elimination of A_T, calculating its input data would be much easier.

$$a^- = \left\{(Q_W + 0.5661) \times \frac{0.93867}{\alpha_c} + 6 \times {Q_W}^3\right\} \times \left\{0.948471 + {Q_W}^2 + 0.5661 \times Q_W\right\} \quad (21)$$

Table 9: Statistical investigation of proposed equations for a^-

Equations	R^2	SAE	MAPE
Equation presented for a^- [Eq. (21)]	0.974	26.4	9.03

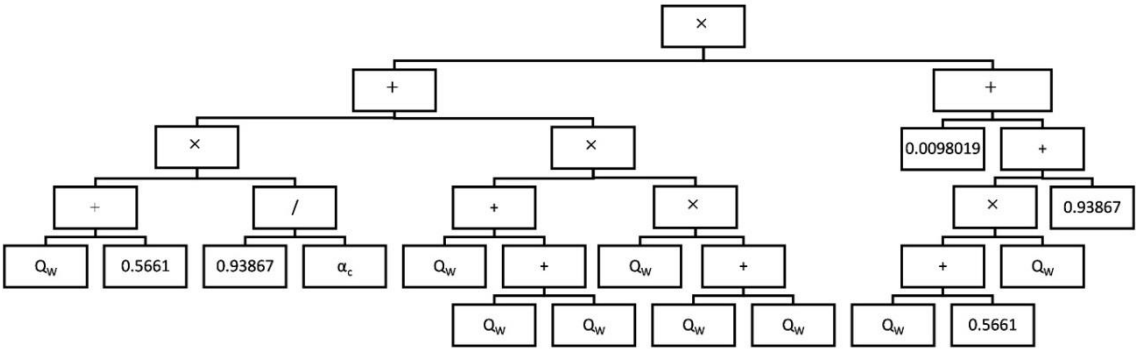

Figure 14. Tree diagram of GP output result for a^-

REFERENCES

1. Kotsovos M, Newman J. Behavior of concrete under multiaxial stress, *J Proceed* 1977; **9**: 443-6.
2. Karsan ID, Jirsa JO. Behavior of concrete under compressive loadings, *J Struct Div* 1969; **95**(12): 2543-64.
3. Kupfer H, Hilsdorf HK, Rusch H. Behavior of concrete under biaxial stresses, *J Proceed* 1969; **8**: 656-66.
4. Reinhardt HW, Cornelissen HA, Hordijk DA. Tensile tests and failure analysis of concrete, *J Struct Eng* 1986; **112**(11): 2462-77.
5. Ren X, Yang W, Zhou Y, Li J. Behavior of high-performance concrete under uniaxial and biaxial loading, *ACI Mater J* 2008; **105**(6): 548-57.
6. Ren X, Yang W, Zhou Y, Li J. Behavior of high-performance concrete under uniaxial and biaxial loading, *ACI Mater J* 2008; **105**(6): 548-57.
7. Huo HY, Cao CJ, Sun L, Song LS, Xing T. Experimental Study on Full Stress-Strain Curve of SFRC in Axial Tension, *Appl Mech Mater, Trans Tech Publ* 2012; **238**(41-45).
8. Babu R, Benipal G, Singh A. Constitutive modelling of concrete: an overview, *Asian J Civil Eng (Building and Housing)* 2005; **6**: 211-46.
9. Tao X, Phillips DV. A simplified isotropic damage model for concrete under bi-axial stress states, *Cement Concr Compos* 2005; **27**(6): 716-26.
10. Lee J, Fenves GL. Plastic-damage model for cyclic loading of concrete structures, *J Eng Mech* 1998; **124**(8): 892-900.
11. Jason L, Huerta A, Pijaudier-Cabot G, Ghavamian S. An elastic plastic damage formulation for concrete: Application to elementary tests and comparison with an isotropic damage model, *Comput Meth Appl Mech Eng* 2006; **195**(52): 7077-92.
12. Wu JY, Li J, Faria R. An energy release rate-based plastic-damage model for concrete, *Int J Sol Structu* 2006; **43**(3): 583-612.
13. Al-Rub RKA, Voyiadjis GZ. Gradient-enhanced coupled plasticity-anisotropic damage model for concrete fracture: computational aspects and applications, *Int J Dam Mech* 2008; **18**(2): 115-54.
14. Voyiadjis GZ, Taqieddin ZN. Elastic plastic and damage model for concrete materials: Part I-Theoretical formulation, *Int J Struct Chang Sol* 2009; **1**(1): 31-59.

15. Taqieddin ZN, Voyiadjis GZ, Almasri AH. Formulation and verification of a concrete model with strong coupling between isotropic damage and elastoplasticity and comparison to a weak coupling model, *J Eng Mech* 2011; **138**(5): 530-41.
16. Sima JF, Roca P, Molins C. Cyclic constitutive model for concrete, *Eng Struct* 2008, **30**(3): 695-706.
17. Wardeh MA, Toutanji HA. Parameter estimation of an anisotropic damage model for concrete using genetic algorithms, *Int J Damage Mech* 2015; 26(6): 801-25.
18. Moradi M, Bagherieh AR, Esfahani MR. Damage and plasticity constants of conventional and high-strength concrete, Part I: Statistical optimization using genetic algorithm, *Int. J. Optim. Civil Eng* 2018; **8**(1): 77-97.
19. Moradi M, Bagherieh AR, Esfahani MR. Relationship of tensile strength of steel fiber reinforced concrete based on genetic programming, *Int J Optim Civil Eng* 2016; **6**(3): 349-63.
20. Koza JR. *Genetic Programming: on Tthe Programming of Computers by Means of Natural Selection*, MIT Press, 1992, **1**.
21. Chen L. Study of applying macroevolutionary genetic programming to concrete strength estimation, *J Comput Civil Eng* 2003; **17**(4): 290-4.
22. Davidson J, Savic DA, Walters GA. Symbolic and numerical regression: experiments and applications, *Inform Sci* 2003; **150**(1): 95-117.
23. Zhang Y, Bhattacharyya S. Genetic programming in classifying large-scale data: an ensemble method, *Inform Sci* 2004; **163**(1): 85-101.
24. Silva S, Almeida J. GPLAB-a genetic programming toolbox for MATLAB, *Proceedings of the Nordic Matlab Conference* 2003, Citeseer, pp. 273-278.
25. Baker JE. Adaptive selection methods for genetic algorithms. *Proceedings of an International Conference on Genetic Algorithms and Their Applications*, Hillsdale, New Jersey, 1985, pp. 101-111.
26. Li J, Ren X. Stochastic damage model for concrete based on energy equivalent strain, *Int J Solids Struct* 2009; **46**(11): 2407-19.
27. Ali AM, Farid B, Al-Janabi A. Stress-Strain Relationship for concrete in compression made of local materials, *Eng Sci* 1990; **2**(1).
28. Dahl KK. Uniaxial stress-strain curves for normal and high strength concrete, Afdelingen for Baerende Konstruktioner, Danmarks Tekniske Højskole, 1992
29. Carreira DJ, Chu KH. Stress-strain relationship for plain concrete in compression, *J Proceed* 1985; 6: 797-804.
30. Muguruma H, Watanabe F. Ductility improvement of high-strength concrete columns with lateral confinement, *Proceedings of the Second International Symposium on Utilization of High-Strength Concrete* 1990; pp. 20-23.
31. Sinha B, Gerstle KH, Tulin LG. Stress-strain relations for concrete under cyclic loading, *J American Concr Institute* 1964; **61**(2): 195-211.
32. Meng Y, Chengkui H, Jizhong W. Characteristics of stress-strain curve of high strength steel fiber reinforced concrete under uniaxial tension, *Jo Wuhan University Technol-Mater Sci Edition* 2006; **21**(3): 132-7.
33. Yan D, Lin G. Experimental study on concrete under dynamic tensile loading, *J Civil Eng Res Pract* 2006; **3**(1): 1-8.

34. Akita H, Koide H, Tomon M. Uniaxial tensile test of unnotched specimens under correcting flexure. Aedificatio Publishers, *Fract Mech Concr Struct* 1998; 1: 367-375.
35. Gopalaratnam V, Shah SP. Softening response of plain concrete in direct tension, *J Proceed* 1985; **3**: 310-23.
36. Zhang Q. Research on the stochastic damage constitutive of concrete material. Ph. D, Dissertation, Tongji University, Shanghai, China, 2001
37. Li Z, Kulkarni S, Shah S. New test method for obtaining softening response of unnotched concrete specimen under uniaxial tension, *Experiment Mech* 1993; **33**(3): 181-8.
38. Ahmad SH. Behavior of hoop confined concrete under high strain rates, *ACI J* 1985; **82**: 634-47.